STUDIA UBB CHEMIA, LXX, 2, 2025 (p. 191-210)
(RECOMMENDED CITATION)
DOI:10.24193/subbchem.2025.2.13

EXPERIMENTAL STUDY ON THE CRYSTALLIZATION FORMATION MECHANISM OF BLIND PIPE IN WUJIAYUAN TUNNEL

Haiting WANG[a,c], Haifeng XU[a], Pengfei HUO[a], Zhuangzhuang WANG[a], Jiqiang YUE[b], Zheng WANG[b], Di ZHANG[c], Tianzhi YU[c,*]

ABSTRACT. In the construction of high-speed railway tunnels, when passing through different geological areas, the groundwater flowing through the drainage blind pipe is easy to produce crystals to block the drainage pipe. These crystal blockages are mainly produced by the dissolution of the concrete material of the initial support of the tunnel, which leads to the accumulation of precipitates in the drainage system and affects the tunnel structure safety. Based on the study of crystals and water samples in the blind pipe of Wujiayuan Tunnel, this paper discusses the relationship between the crystals in the blind pipe and the ion concentration, pH value, carbon dioxide concentration and partial pressure and temperature in groundwater. Combined with the environmental water chemical equilibrium software Visual MINTEQ 3.1, the influence of the above conditions on the formation of crystallization was simulated and the formation mechanism of Wujiayuan tunnel blind tube crystallization was proposed.

Keywords: *tunnel blind pipe, crystals, water samples, Visual MINTEQ 3.1, precipitation formation mechanism*

INTRODUCTION

With the rapid development of high-speed railroad projects in China, tunnel blind crystallization has become a major challenge for Chinese engineers

---

[a] *The 6th Engineering Co., Ltd. of China Railway, 3th Bureau Group, 710000, China.*
[b] *Xi'an Chengdu Railway Passenger Dedicated Line Shaanxi Co., Ltd, Xi'an, 710000, China.*
[c] *Lanzhou Jiaotong University, Lanzhou 730070, China.*
[*] *Corresponding author: yutzh@mail.lzjtu.cn*

during tunnel construction. The Wujiayuan Tunnel is located in the northern part of China's Shanxi Province, where the terrain is complex and varied. The local water is rich in calcium ions (Ca^{2+}), which tend to crystallize and deposit on the tunnel walls. This deposition usually leads to blockage and jeopardizes the load-bearing capacity of the tunnel; therefore, it is crucial to study the formation mechanism of tunnel crystallites.[1-4]

The crystallization process of groundwater is a series of complex chemical reactions. The main components of the crystalline substances in the tunnel groundwater are insoluble carbonates and calcium salts mainly composed of calcium carbonate. The key to solving the problem of calcium carbonate crystallization blocking the pipeline is to clarify the mechanism of calcium blocking. Studies have shown that calcium carbonate crystals are solid substances arranged continuously in space according to a certain regularity, and the crystallization process is carried out in stages, and the crystallization morphology is different at different stages [5]. Bobet et al.,[6] investigated and quantified the crystallization blockage in the drainage system of Nanla Tunnel, revealed its formation mechanism, and explored the effectiveness and applicability of coatings in preventing crystallization blockage. Jiang et al. [7] investigated the crystallization of the Nanla Tunnel drainage system. the crystalline clogging in the drainage system, of Nanla tunnel and found that the crystalline clogging was mainly composed of calcium carbonate and a small amount of sediment and cement hydration products, and the formation of crystals was a result of the corrosive effect of the groundwater on the shotcrete. Yan et al [8] investigated the mixing of calcium carbonate and calcium sulphate in the scaling precipitation, which was frequently observed in the extracted water supply due to the treatment process. The results of co-precipitation were compared with the experimental results of single salt crystallization, and several parameters, such as conductivity, pH, crystal morphology and crystal shape, were carefully monitored to study the crystallization mechanism. Liu et al [9] used mathematical modeling to synthesize and analyze the mechanism of flocking and anti-clogging of drainage pipes. Zhou et al [1] measured the flow rate of a calcium carbonate crystal tunnel in a southwestern mountainous area. Numerical simulation was combined with finite element software (ANSYS Fluent) based on the actual flow results. The crystallization of calcium carbonate near the interface of the tunnel drain and the formation mechanism were analyzed. Feng et al [10] investigated calcium ion deposition in the presence of different sources of PCC to reveal the influencing factors and mechanisms of $CaCO_3$ nucleation and crystal growth. Chen et al [11] examined the crystals by using EDS, Scanning Electron Microscope (SEM), and XRD [12-18] to analyze the elemental compositions, material composition and microstructure. Finally, a measure to remove crystals from tunnel drains using ultrasound was proposed.

Groundwater seepage through the initial support concrete is alkaline environment, which provides the basis for the formation of crystals, and CO_2 is dissolved in groundwater, which is easy to react with Ca^{2+} to form precipitates under alkaline environment. This paper analyzes the relationship between the crystals in the blind pipe and the ion concentration, pH value, CO_2 concentration and partial pressure and temperature in the groundwater, and summarizes and researches the formation mechanism of the crystals in the blind pipe by using Visual MINTEQ 3.1, which can be used to analyze the relationship between the crystals in the blind pipe and the ion concentration and partial pressure and temperature in the groundwater.

RESULTS AND DISCUSSION

Analysis of Ion Concentration in Water Seepage from the Wujiayuan Tunnel

The groundwater in the tunnel area exhibits a diverse array of ions, including Ca^{2+}, Mg^{2+}, Ba^{2+}, CO_3^{2-}, HCO_3^-, OH^-, and SO_4^{2-}. These ions significantly influence the crystallization processes within the tunnel's groundwater. Additionally, ions such as Cl^- and Na^+ play a role as well. The introduction of NaCl into carbonate solutions induces an ionic strength effect, resulting in an influx of Na^+ ions due to NaCl's high solubility, the increase of ionic strength has an effect on the solubility of carbonate.

To investigate the ion concentrations in the seepage water from the Wujiayuan Tunnel, we collected samples from various locations: the outer layer of the exit shotcrete, the outer layer of shotcrete from Well 3, drainage water from Well 3, and water samples from different positions within the surrounding rock of the inclined Well 3, as well as leachate from the sprayed concrete. A total of eight samples were obtained. Additionally, we conducted ion concentration tests on the leachates from the construction materials used in the Wujiayuan Tunnel, such as cement and fly ash [11]. The specific data for the leachate from the shotcrete at the tunnel exit is illustrated in the figure below [12].

Through the analysis of the data presented, it is evident that two samples were taken from the leachate of the shotcrete outer layer at the exit of the Wujiayuan Tunnel. Additionally, one sample was collected from the drainage pipe of shotcrete at Shafts No.3, and one sample each from the surrounding rock water at Shaft No.3, tunnel exit surrounding rock water, and leachate from the shotcrete. The second sampling of the leachate from the shotcrete outer layer at the tunnel exit occurred post-application. The provided data indicates that the Na^+ concentration remained relatively stable, while the Ca^{2+} concentration increased by approximately threefold. Furthermore, the Mg^{2+} content surged by 30 mins. The cause may be linked to water flowing along the outer perimeter of the tunnel after passing through the shotcrete, which leads to the leaching of significant amounts of Ca^{2+} and Mg^{2+} from the surface of the shotcrete. The concentrations of sodium ions in the leachate from the three batches of fly ash, the shotcrete leachate from Wujiayuan, and the surrounding rock water at the tunnel exit showed fluctuations between 2 to 10 times compared to other samples. Given that the sodium ion concentration in the three batches of fly ash leachate reached 159 mg/L, it is reasonable to deduce that the increase in sodium ion concentration in the shotcrete leachate and the surrounding rock water at the tunnel exit is associated with the fly ash used in the construction process.

Table 1. The water seepage and ion concentration of various sections of WujiaYuan Tunnel

Sample name	Ion content mg/L					
	Na^+	Ca^{2+}	Mg^{2+}	CO_3^{2-}	HCO_3^-	SO_4^{2-}
Water seepage through the concrete outer layer at the tunnel exit of the Wujiayuan tunnel	42.3	6.34	0.185	no detection	176.6	71.6
Two samples of the Wujiayuan tunnel	44.1	19	31.5	8.8	211.9	99.2
No. 3 inclined shaft blowout concrete outer drainage pipe leaching water	47.5	5.74	1.37	no detection	118.4	99.4
No. 3 Shakai Rock Water	54.6	15.3	19.8	6.8	214.3	69.5
Wujiayuan exit tunnel surrounding rock water	760	5.12	1.61	110.0	594.2	237
Three rounds of cement leaching water	71	409	0.484	no detection	140.6	1.62×10^3
Three rounds of fly ash leaching water	159	465	0.588	no detection	130.2	1.23×10^3
Wujiayuan shotcrete leaching water	183	28.5	0.682	3.2	65.8	509

The data from the table 1 indicates that the Ca^{2+} concentration in the first sampling was relatively low. In contrast, the concentrations of Ca^{2+} and Mg^{2+} in the second sampling exhibited a significant increase compared to the first. This difference may stem from the initial stage of groundwater seepage, where the water had insufficient contact with the concrete, resulting in minimal transport of calcium and magnesium. As the duration of groundwater seepage increased, the interaction between groundwater and concrete intensified, leading to a greater release of cations.

In the leachate tests of cement and fly ash construction materials, significant levels of calcium ions were detected, with concentrations reaching 409 mg/L and 465 mg/L. However, the absence of CO_3^{2-} ions suggests that the primary source of anions in carbonate crystals relates to CO_2. This observation confirms that groundwater flowing through tunnel surrounding rock layers leads to the formation of substantial crystalline structures upon discharge from blind pipes. Notably, the concentrations of HCO_3^- and SO_4^{2-} ions were higher than those of other ions, which likely explains why carbonate and sulfate dominated in the formed crystals.

Analyzing the first three sets of provided data reveals that sodium ion concentrations remained relatively constant. However, the leachates from the fly ash and pumped concrete, as well as the surrounding water at the tunnel exit, exhibited sodium ion concentrations that were 2 to 10 times higher than those of other samples. Given that the sodium ion concentration in the fly ash leachate reached 159 mg/L, and the sample sourced from the surrounding rock utilized fly ash that was sprayed during construction, it is reasonable to associate the elevated sodium ion concentrations in the sprayed concrete leachate and tunnel exit water with the presence of fly ash.

The primary cause of crystal formation in blind pipes stems from the significant interaction between abundant calcium ions in groundwater and construction materials like cement and fly ash, along with CO_2 from water and air. The accumulation of crystals within blind pipes poses a threat to tunnel lining structures and drainage systems. A prominent issue arising from this is crystallization, which obstructs the drainage systems, leading to drainage failure. This results in the lining structures experiencing elevated external water pressure, thereby jeopardizing the structural integrity of the tunnel. Consequently, this may lead to cracks and subsequent leaks, severely affecting the safe operation of the tunnel.

XRD analysis of crystallites in Wujiayuan tunnel

In order to further explore the chemical composition of the crystalline substance of the tunnel blind tube, water samples were collected at the tunnel construction site, and the crystalline substance of the blind tube was tested and analyzed by XRD (as shown in Figure 1~2). It can be seen from Figure 2(a) that the horizontal coordinate is the Angle formed between the direction of the reflected diffraction beam at the crystalline edge of Wujiayuan

Tunnel and the direction of the incident beam, and the vertical coordinate represents the crystallization peak intensity of Wujiayuan tunnel. The location of the main peak of tunnel crystallization is the same as that of JCPDS file 97-001-6710 in the crystal Structure and diffraction database. The X-ray diffraction spectra show different diffraction peaks, angular positions and relative intensity changes, indicating that the composition elements of the crystal materials are different. Based on equations (1) ~ (2), the mass fraction of each phase within the substance was calculated.

$$\frac{\omega_i}{\omega_j}=\frac{I_i K^{j}_{Al_2O_3}}{I_j K^{i}_{Al_2O_3}} \tag{1}$$

$$\omega_i+\omega_j=1 \tag{2}$$

According to the XRD fitting curve shown in Figure 1, the maximum diffraction peak is located at 2θ= 29.178 °, and the crystal face index is (104) corresponding to the #86-2341 calcite standard card, whose content accounts for 82% of the crystallite mass ratio in Wujiayuan Tunnel. The maximum diffraction peak is located at 2θ= 29.499°, the crystal surface index is (104) corresponding to the #89-1304 high magnesium calcite standard card, and its content accounts for 18% of the mass ratio of crystallites in Wujiayuan Tunnel. The standard XRD spectra of the two crystal types are shown in Figure 2(b).

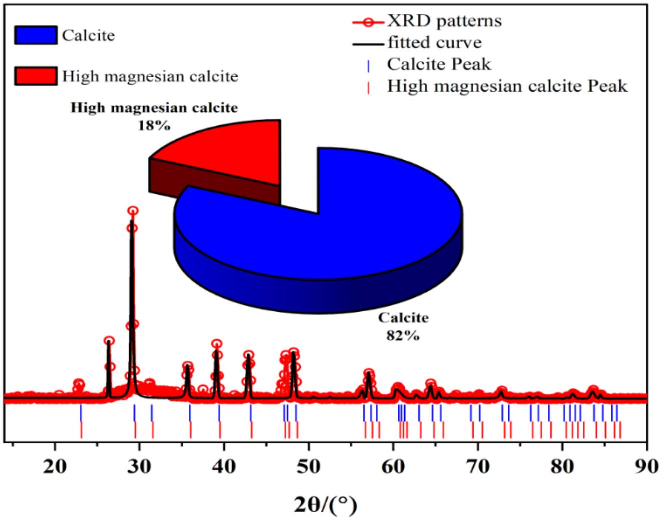

Figure 1. XRD pattern fitting analysis

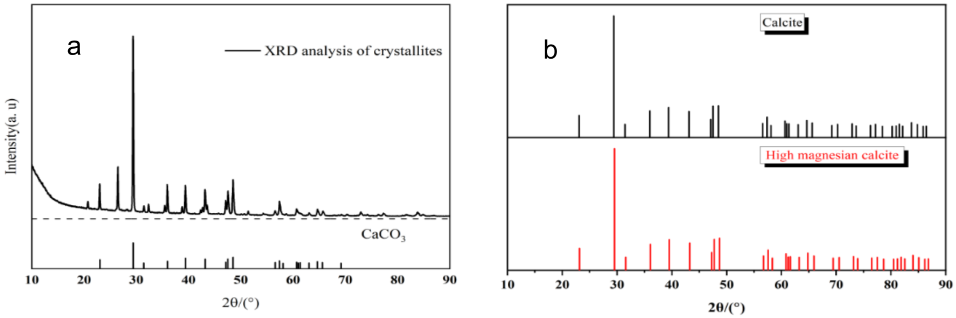

Figure 2. Tunnel XRD pattern and standard XRD diffraction spectrum of each crystal type

Calculation and simulation of the effect of pH on precipitation saturation index

In order to clarify the cause and mechanism of crystal formation in tunnel drainage system, the influence factors of crystal formation and precipitation equilibrium process in tunnel were simulated by simulation software Visua I MINTEQ (Figure 3). The mathematical expression of SI is:

$$SI = \lg(IAP/K_{sp}) \tag{3}$$

In the formula, IAP (ion activity product) is the product of ion activity in solution, that is, ion product; K_{sp} is the activity product constant (solubility product constant) of insoluble compounds at a specific temperature, which is a function of temperature and has nothing to do with the initial ion concentration. When IAP > K_{sp}, SI > 0, the substance is supersaturated, it will precipitate; The ion concentration has a direct and significant effect on the precipitation saturation index of calcium carbonate. As shown in Figure 3, firstly, the calcium ion distributions containing carbonates under different pH are calculated (Figure 3a). It can be seen that the contribution of carbonate to precipitation is greater, which is consistent with the test results of crystalline precipitation samples. The main precipitate component is calcium carbonate. Due to the high solubility of calcium ions, it forms mixed precipitation with $CaCO_3$ when it is supersaturated. The ion concentration in the surrounding rock water of the tunnel is HCO_3^- > Ca^{2+} > CO_3^{2-} from high to low. Among them, the content of HCO_3^- is higher, which is 214.3 mg/L. The concentration of calcium ion is high, and the concentration of CO_3^{2-} ion does not reach the detection limit, indicating that the crystals precipitated in the karst tunnel drainage pipe are mainly produced by chemical reaction under the condition of solubility change. In the range of low pH, there is only HCO_3^- and CO_2 in water. There are only CO_3^{2-} ions in the higher pH range. HCO_3^- dominates in the range of medium pH values. Therefore, when the pH of water is high, the precipitation amount of calcium carbonate increases; on the contrary, when the pH value of water is low, calcium carbonate is not easy to precipitate (Figure 3b). When the pH is 0-10, the precipitation formation rate continues to increase, but when the pH is more than 10, the precipitation formation rate tends to slow down. At room temperature, the higher the pH, the greater the saturation index of $CaCO_3$. When $pH > 8.1$, $CaCO_3$ precipitates gradually. This is due to the fact that the concentration of Ca^{2+} in the open system increases with the increase of pH, which makes the ion product of $CaCO_3$ increase gradually. This is due to the fact that the concentration of Ca^{2+} in the open system increases with the increase of pH, which makes the ion product of $CaCO_3$ increase gradually. The trend curve of the saturation index of $CaCO_3$ in the open system with temperature change in the temperature range of 20.0 - 26.0 °C at $pH = 8.1$ was drawn according to the convergence data (Figure 3c). With the increase of temperature, the saturation index of $CaCO_3$ increases, and the critical temperature of $CaCO_3$ precipitation is about 25.0 °C. This is because the solubility of $CaCO_3$ in the solution decreases with the increase of temperature, that is, more $CaCO_3$ will be precipitated when the water temperature increases. According to the simulation data, the pH when the saturation index was reached at 1 times carbon dioxide partial pressure, 1.5 times carbon dioxide partial pressure, and 2 times carbon dioxide partial pressure was summarized. As shown in Figure 3d, it can be found from the figure that as the partial pressure of CO_2 increases, the content of CO_2 in the gas phase gradually increases. According to Henry 's law, the content of CO_2 in the liquid phase will also increase accordingly, resulting in more carbonic acid. The pH value of the solution is reduced, and the calcium carbonate precipitation is easily dissolved under acidic conditions, thus reducing the deposition rate of calcium carbonate. From the diagram, it can also be found that the critical pH of calcium carbonate precipitation is 8.1 under the condition of 1 times the partial pressure of carbon dioxide. Under the condition of 1.5 times of carbon dioxide partial pressure, the critical pH of calcium carbonate production precipitation is 7.9 ; under the condition of 2 times carbon dioxide partial pressure, the critical pH of calcium carbonate production precipitation is 7.8.

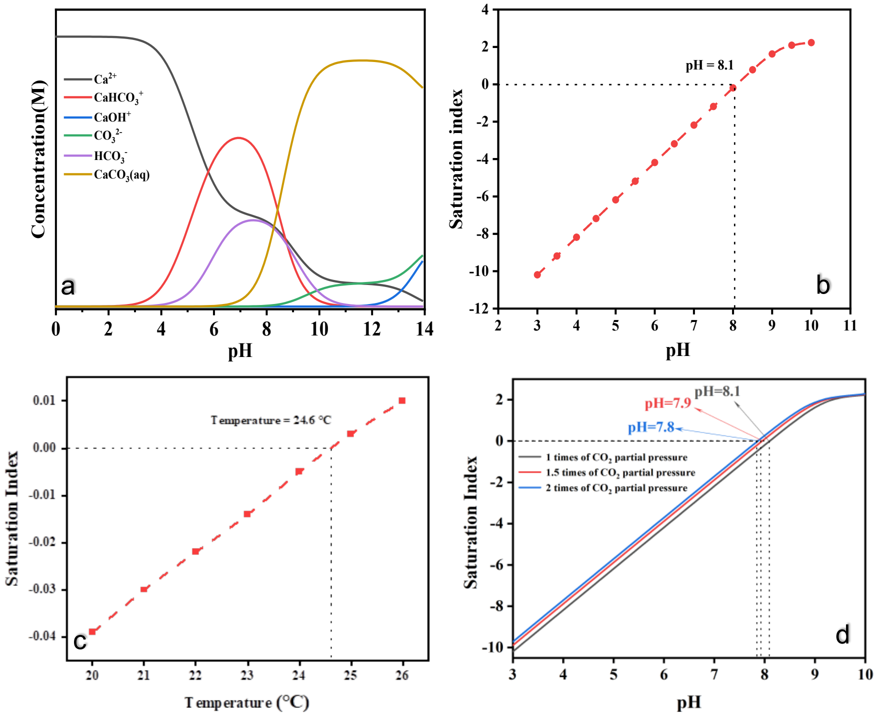

Figure 3. The influence of various factors on the saturation index is calculated and simulated (a. The precipitation mechanism of Ca^{2+} in water as the pH changes. b. Effect of pH on saturation Index of calcium Carbonate. c. Saturation index of $CaCO_3$ changing with temperature. d. Effect of pH on the saturation index of calcium carbonate.)

pH influence experiment analysis

While keeping other factors the same and unchanged, we set different pH gradients, observed and recorded the crystallization of the experimental solution under different pH environments, studied and analysed the effect of pH on the crystallization blockage of tunnel blind pipes, and provided guidance for the control of environmental pH during tunnel maintenance. The crystallization quality of experimental water samples under different pH conditions is shown in the figure below.

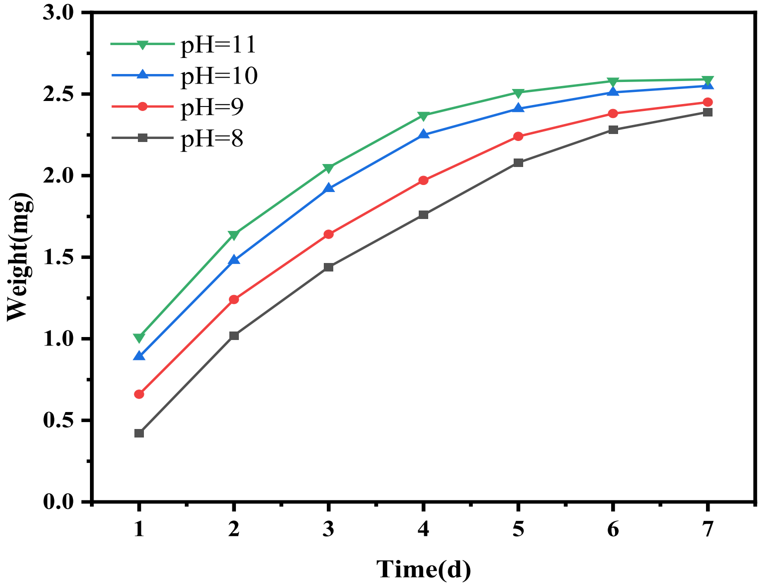

Figure 4. Relationship between time and crystal quality in different pH environments

It can be seen from Figure 4 that the reaction rates of the experimental solutions are different in different pH environments after a complete experiment lasting about one week. Taking pH equal to 8 as the research point, in the environment of high pH, the crystal formation rate is faster in the early stage, and tends to be slower in the middle and later stage, while in the alkaline environment with lower pH, the reaction rate of the experimental solution is relatively small, and the crystal quality increases slowly, but in the later stage, the solution is faster in the pH environment with higher crystal formation rate. The reason for the analysis may be that there is little difference in the content of $Ca^{2+}$and Mg^{2+} in the whole experimental solution and there is no follow-up supplement with the experimental reaction, which leads to the relatively large pH value of the experimental environment in the middle and later stage, but the ion concentration is low, so the reaction rate becomes slower. At the end of the experiment, the quality of crystals formed in different pH solutions is about the same, indicating that Ca^{2+} and Mg^{2+} in the experimental solution react with CO_3^{2-} and SO_4^{2-} to form carbonates and sulfates.

It can be seen that the pH value has a great influence on the solubility of calcium carbonate precipitates. When the pH is closer to 8, the crystallization rate is slower, and when the pH is further increased, the crystallization rate becomes faster, so in the actual tunneling operation, the solution pH should be kept near 8 as far as possible.

Experimental study on the effect of different ionic strength on the crystallization of tunnel blind tube

Referring to the on-site water sample analysis report and various literature data, the initial concentrations of Ca^{2+} ions and HCO_3^- should be set at higher levels to prevent excessive experimental error due to low initial concentrations. The production of crystallization in weakly alkaline solutions relates to the concentrations of Ca^{2+} and HCO_3^-. However, calcium bicarbonate easily decomposes into $CaCO_3$, and a single reagent cannot adjust the concentrations of different ions. Therefore, it is not feasible to directly prepare a solution using solid calcium bicarbonate; instead, $CaCl_2$ and $NaHCO_3$ are used to prepare the experimental solution. The experimental results and analysis are as follows, with specific experimental procedures detailed in the section on factors influencing calcium carbonate crystallization.

The reaction temperature is 25 °C, the pH is adjusted to 8.1 with borax solution, the beaker is open, the initial concentration of bicarbonate is 50 mg/L, and the initial concentration of Ca^{2+} ion is changed. The experimental results are shown in Figure 5.

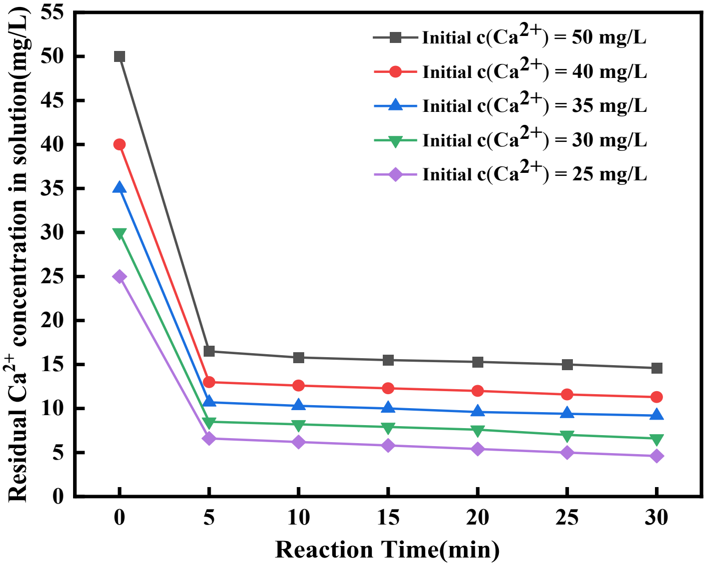

Figure 5. Variation of Ca^{2+} ion concentration with reaction time under different initial Ca^{2+} ion concentration

It can be seen from Figure 5 that with the increase of the initial Ca^{2+} ion concentration, the slope of the Ca^{2+} ion concentration curve of 5 min before the reaction also increases, from 3.68 mg/ (L·min) when the initial

Ca^{2+} ion concentration is 25 mg/L to 5.40 mg/ (L·min) when the initial Ca^{2+} ion concentration is 50 mg/L. The curve fluctuates slowly within 25 min after the reaction, because the formation and dissolution of $CaCO_3$ is a slow and reversible process with the participation of CO_2 and H_2O.

Bicarbonate first dissociates, and the resulting CO_3^{2-}reacts with Ca^{2+} in the solution to form $CaCO_3$ crystals. The HCO_3^-produced by hydrolysis is unstable and is easily decomposed into CO_2 and H_2O, the reaction of $CaCO_3$, CO_2 and H_2O to form water-soluble $Ca(HCO_3)_2$. When the initial Ca^{2+} ion concentration is not high, the Brownian motion of the particles in the solution is slow and the reaction rate is slow. Increasing the initial Ca^{2+} ion concentration increases the collision probability between particles and increases the reaction rate. It can be seen from the reaction formula that increasing the initial Ca^{2+} ion concentration can promote the reaction equilibrium to shift to the right and increase the overall reaction rate.

Table 2. Crystallization rate after reaction for 30 min
at different initial Ca^{2+} concentrations

Initial Ca^{2+} concentration (mg/L)	50	40	35	30	25
Crystallization rate W (%)	4.00	4.05	3.05	2.39	0.31

Table 2 shows the crystallization rate (W) after the reaction of 30 min with different initial Ca^{2+} ion concentrations. The formula for calculating the crystallization rate is as follow: $W=\frac{\Delta m}{A}\times\Delta t$. In the equation, Δ_m refers to the mass of crystals formed during the crystallization process. A denotes the surface area available for crystal growth, which typically depends on the shape and size of the crystals. Δ_t indicates the duration from the onset of nucleation to the point at which the crystals reach a specified size. The crystallization rate increases with the increase of the initial Ca^{2+} ion concentration. It can be seen from the reaction formula that the increase of Ca^{2+} ion concentration can make the reaction proceed to the left and inhibit the dissolution of calcium carbonate.

The effect of CO_2 on the formation of tunnel crystals

CO_2 plays a vital role in the formation of precipitated crystals in the tunnel drainage pipe. CO_2 dissolves in water to form carbonic acid (H_2CO_3), and carbonic acid can be ionized in water. The ionization equation is shown in Equation (3):

$$H_2CO_3 \rightarrow H^{+} + HCO_3^{-} \qquad (3)$$

When [H^+] = 3×10^{-7}mol / L, the concentration of H_2CO_3 is equal to the concentration of HCO_3^-, and the aqueous solution is in equilibrium, that is, there is neither precipitation crystallization nor dissolution. When [H^+] > 3×10^{-7}mol / L, the precipitation and crystallization of calcium carbonate and magnesium carbonate will occur. The precipitated crystals in the tunnel drainage pipe are mainly precipitated by the precipitated crystals formed and dissolved by the chemical reaction in the case of solubility changes. The chemical equation for the precipitate crystals formed by the chemical reaction is as follows:

$$Ca^{2+} + Ca(OH)_2 + 2\ HCO_3^{-} \rightarrow 2\ CaCO_3\downarrow + 2\ H_2O \qquad (4)$$

$$Mg^{2+} + 2\ HCO_3^{-} \rightarrow MgCO_3\downarrow + CO_2\uparrow + H_2O \qquad (5)$$

$$Ca^{2+} + SO_4^{2-} \rightarrow CaSO_4 \qquad (6)$$

By observing the above chemical reaction equations, it is not difficult to find that CO_2 plays a very important role in the formation of precipitated crystals in the tunnel drainage pipe. When the tunnel is excavated, the gas partial pressure of CO_2 in the groundwater will decrease, resulting in a decrease in the solubility of CO_2 in the groundwater. The dissolved CO_2 escapes from the groundwater solution, resulting in a chemical reaction in the direction of the formation of precipitated crystals. The dissolved Ca^{2+} and Mg^{2+} in the aqueous solution are precipitated in the form of insoluble carbonates, and the crystalline precipitates in the groundwater solution tend to be saturated. The carbonates precipitated from the aqueous solution will adhere to the wall of the tunnel drainage pipe, resulting in an increase in the wall friction of the tunnel drainage pipe. The movement of the groundwater flow becomes more and more significant, which ultimately leads to the weakening of the water conveyance capacity of the tunnel drainage pipe.

Experiment on the effect of CO_2 on tunnel crystallization

The experimental part of the effect of CO_2 on tunnel crystallization is presented in the following sections. Analysis of comparative experimental results of sealed and unsealed under indoor conditions. The crystallization quality of the solution under different CO_2 contact modes is shown in Table 3.

Table 3. Experimental results of the effect of CO_2 on crystallization

Time (d)	Quality of unsealed crystalline water sample (mg)	Quality of sealed crystalline water sample (mg)
1	0.0500	0.0169
2	0.1025	0.0206
3	0.1427	0.0241
4	0.1762	0.0263
5	0.2049	0.0282
6	0.2336	0.0300
7	0.2581	0.0314

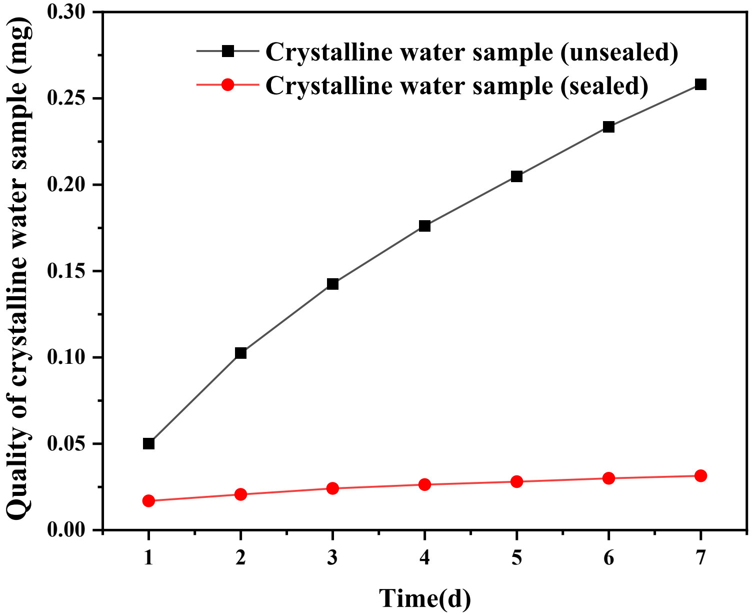

Figure 6. The effect of CO_2 on the crystallization of water samples in tunnel site under indoor conditions

Figure 6 shows the effect of CO_2 on the crystallization of water samples in the tunnel site under sealed and unsealed conditions under indoor conditions. It can be seen from the figure that the crystal quality generated when the experimental water sample in the beaker is in full contact with the air is larger than that when the seal is not in contact with the air, and the amount of crystallization gradually increases. With the increase of CO_2 contact time, the deposition rate of calcium carbonate gradually decreases. The reason is that with the increase of CO_2 contact time, CO_2 in the gas phase is continuously supplemented, and the content of CO_2 in the liquid phase will increase accordingly, resulting in more carbonate ions and the formation of calcium carbonate precipitation. At the same time, with the increase of calcium carbonate deposition, the concentration of Ca^{2+} ions gradually decreases, so that the deposition rate of calcium carbonate gradually decreases.

The experimental results show that CO_2 has a great effect on the crystallization of tunnel water samples, as shown in Table 3 and Figure 6. In the beaker in contact with air, the maximum crystallization amount was 0.258 mg after 7 days, while in the sealed tunnel water sample, the maximum crystallization amount was only 0.031 mg after 7 days. At the same time, according to the image, the effect of CO_2 on the amount of crystallization is a significant trend in the early stage and a gentle trend in the later stage. That is, in the first 5 days of the experiment, the amount of crystallization increases rapidly, while in the 6-7 days, the amount of crystallization increases slowly. The reason may be that the corresponding Ca^{2+} and Mg^{2+} are consumed during the crystallization process, resulting in insufficient ion concentration in the later stage and a decrease in the crystallization rate, which is in line with the deposition rate of $CaCO_3$.

Effect of temperature on the formation of tunnel crystals

The effect of temperature on the formation of precipitated crystals in the tunnel drainage pipe is also very significant. According to statistics, under normal atmospheric pressure, when the water temperature is 5 ^{o}C, the solubility of $CaCO_3$ is 86 ppm; when the temperature is increased by 10 ^{o}C, the solubility of $CaCO_3$ is reduced to 75 ppm. This indicates that $CaCO_3$ is more likely to approach supersaturation as the temperature of water increases. When the temperature increases, the reaction proceeds in the direction of positive reaction, which is beneficial to the formation of precipitated crystals in the tunnel drainage pipe.

The results of crystallization kinetics study on $CaCO_3$ precipitation crystallization show that the precipitation crystallization process of $CaCO_3$ conforms to the general law of crystallization kinetics, which can be divided into the formation of crystal nucleus and the growth stage of crystal grains. Among them, the solute crystallizes from the solution and needs to go through two stages: in the aqueous solution, tiny particles are first produced as the core of the crystallization, which is called the crystal nucleus, and then the crystal nucleus gradually grows into a visible crystal. The process of nucleation is called nucleation (or nucleation formation). Then, the nucleus gradually grows into micro-grains, which are called grain growth due to the process of continuous contact, collision and growth of micro-grains in solution due to thermal motion (Brownian motion).

The change of temperature conditions will not only lead to the change of the hydrodynamic properties of the aqueous solution and the balance of $CO_2 - CaCO_3$, which will promote the escape of CO_2 dissolved in the aqueous solution, resulting in the acceleration of the precipitation crystallization rate of carbonate rocks, but also directly affect the volume and concentration of the solution. For example, when the temperature increases, the liquid surface of the aqueous solution evaporates, resulting in an increase in the concentration of Ca^{2+} ions in the solution.

Effect of temperature on the formation of calcium carbonate precipitation

Table 4. Crystallization of saturated / unsaturated water samples with temperature

	20 °C	25 °C	30 °C	35 °C
Tunnel saturated water sample	Crystal did not form	White crystals are formed	Suspended liquid appears	The solution becomes clear
Tunnel supersaturated water sample	There is slight crystallization formation.	White crystals are formed	Suspended liquid appears	The solution becomes clear

The specific operation and related conditions of the experiment have been described in detail in the experimental section. It can be seen from the data in the Table 4 that the temperature has an important influence on the crystallization of the tunnel blind tube. In the Wujiayuan tunnel, the temperature has obvious crystallization at 25 °C. As the temperature increases, the solubility of the crystal increases. At 35 °C, the crystal dissolves and the solution is clarified. Therefore, increasing the temperature to about 30 °C can effectively reduce the crystallization of the tunnel blind tube. In the process of dealing with blind tube crystals, it can be considered to increase the temperature to inhibit blind tube crystallization.

Analysis of the formation mechanism of crystals in Wujiayuan tunnel

Combined with the calculation and simulation process of crystals, it can be seen that the crystallization and precipitation of tunnel blind tube are related to the saturation, pH value, temperature, pressure and solution properties of the solution, and the crystallization process is the combined effect of several factors. Changes in ambient temperature, pressure, evaporation, concentration of impurities or any other component in the solution may cause the equilibrium system to be readjusted.

The scaling ions also mainly come from two aspects, one is the groundwater itself (with the rock, etc.), and the other is the dissolution of concrete. There are many kinds of soluble salts in the groundwater of tunnel surrounding rock, such as bicarbonate, sulfate, phosphate, chloride, soluble carbonate and silicate. At the same time, the tunnel shotcrete is rich in calcium salts, and the groundwater seepage brings calcium ions into the tunnel blind tube through shotcrete. When in contact with the air, a large amount of CO_2 is dissolved in water, so that the groundwater contains a large amount of CO_3^{2-}, HCO_3^-, etc., HCO_3^- is unstable and easy to decompose to form CO_3^{2-}. The combination of Ca^{2+} and CO_3^{2-} is easy to form insoluble calcium carbonate. Calcium carbonate crystals are precipitated from water and grow slowly on the inner wall of the blind tube. At the same time, cement and fly ash contain a large amount of silicon dioxide, and the multiple effects of the above situation eventually form blind tube crystallization.

Temperature is another important factor affecting crystal precipitation. The solubility of most salts in water increases with the increase of temperature, but the solubility of the tunnel crystal is abnormal. When the temperature increases, the solubility decreases, that is, more crystals will be precipitated when the water temperature increases. Fig.7 shows the solubility curve of calcium carbonate crystals with temperature. With the increase of temperature, the saturation index of the crystal becomes larger, and the critical temperature for the formation of the tunnel crystal is about 25.0 °C.

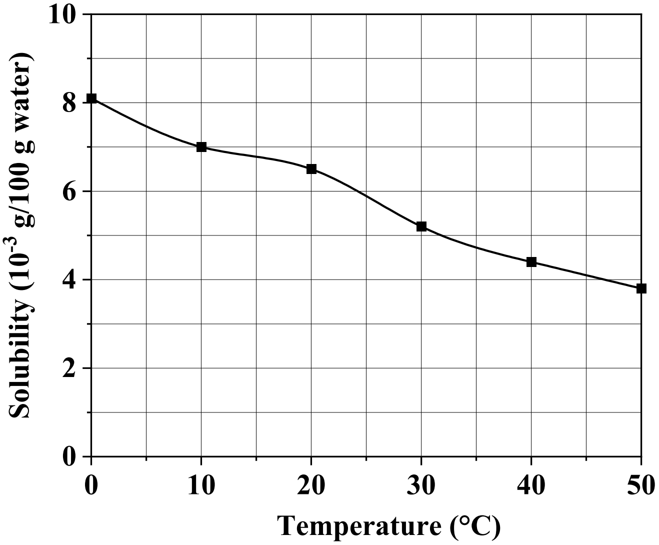

Figure 7. The solubility curve of calcium carbonate crystal changing with temperature

Different pH environments will significantly affect the formation of tunnel fissure water crystals, and change the balance of HCO_3^-, CO_3^{2-}, OH^-, and H^+ in the original solution. Under alkaline conditions, HCO_3^- will be more easily converted into CO_3^{2-}, and then react with Ca^{2+} to form insoluble crystals. The formation mechanism of crystals is shown in Figure 8. In the low pH range, only bicarbonate and carbon dioxide exist in the water. HCO_3^- is dominant in the medium pH range. Only CO_3^{2-} ions are present in the higher pH range. At room temperature, the higher the pH, the greater the saturation index of $CaCO_3$. When pH >8.1, $CaCO_3$ precipitate gradually. This is because the concentration of CO_3^{2-} in the open system increases with the increase of pH, which makes the ion product of $CaCO_3$ gradually increase. High pH water is easy to absorb carbon dioxide and react with calcium ions in the drainage solution, which is the main reason for the scaling of calcium carbonate, calcite and aragonite. There are two main reasons for the high pH value in water. One is the increase of pH value caused by concrete reaction. Second, part of the groundwater itself has a high pH. At the same time, the main cations in the tunnel blind pipe water are Ca^{2+}, Mg^{2+} and Na^+ ions. In this alkaline environment rich in calcium and magnesium ions, Mg^{2+} has a stronger affinity for some sites on the surface of the mineral, so it can replace part of Ca^{2+} into the lattice and eventually form high magnesium calcite. In summary, the crystallization mechanism of the tunnel drainage system is shown in the figure, and the reaction mechanism is summarized as follows:

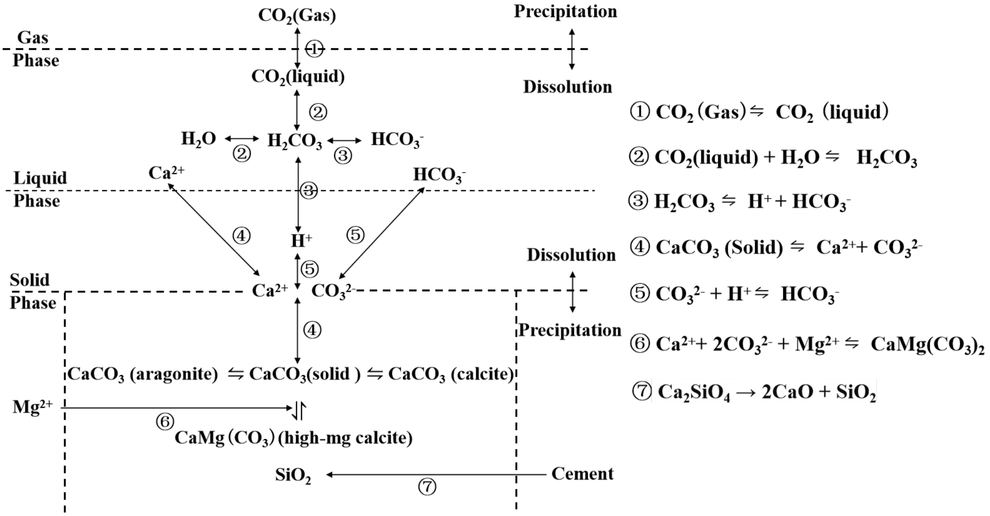

Figure 8. Formation mechanism of calcium carbonate crystallization in tunnel

The fissure water in the surrounding rock of the tunnel penetrates through the shotcrete of the initial support, which will take away a large amount of alkaline substances such as $Ca(OH)_2$, making the water body strongly alkaline. The changes of high temperature, high humidity environment conditions and CO_2 partial pressure in the drainage system lead to the destruction of chemical equilibrium and the rapid crystallization of carbonate. In addition, at present, there are no requirements for the smoothness, smoothness and pollution resistance of the inner wall of the drainage component. Crystals are concentrated on the inner wall surface of the drainage system, and long-term crystallization precipitation blocks the drainage system. Especially when the water flow rate is low, the crystallization time is sufficient, and the drainage system is more likely to be blocked. The crystal of the drainage blind pipe is white and light yellow. In the drainage blind pipe, a uniform deposition layer is formed and deposited on the blind pipe wall at a relatively uniform density. These crystals may gradually increase density under the erosion of water flow. With the passage of time, the sediment will lead to the decrease of the inner diameter of the drainage blind pipe, and poor drainage will occur when the deposition is serious. The deposition of crystals may cause uneven water flow, forming rapid and slow changes in water flow. Turbulence may be more pronounced in the area where crystals accumulate. The bottom or side wall of the drainage ditch is a crystal deposition area, which may visually appear as a granular or uniform crystal layer. Crystals may form granular, massive or aggregated structures on the surface of the drain, and different surface textures may be felt during observation. Many tunnels still produce crystals after 5 years or even 10 years of operation, because cement hydration is a long-term continuous process, and the flowing water has a great influence on the concrete. Under the action of continuous groundwater erosion, the calcium substances in the concrete are continuously dissolved and brought out, so the tunnel faces the potential harm of drainage pipe crystallization blockage for a long time, which is a long and lasting process.

CONCLUSION

In this paper, the water treatment analysis is carried out according to the crystals sampled in the Wujiayuan tunnel. The relationship between the crystal in the blind tube and the ion concentration, pH value, CO2 concentration and partial pressure, temperature in the groundwater was explored. The effect of pH on the precipitation saturation index, the effect of carbon dioxide partial pressure on the precipitation saturation index, the effect of temperature on the precipitation saturation index, and the effect of ionic strength on the precipitation saturation index were simulated by using the environmental water chemical equilibrium software Visual MINTEQ 3.1. The formation mechanism of blind tube crystallization in Wujiayuan tunnel is summarized.

EXPERIMENTAL SECTION

For details of the experimental part, please refer to the Supporting Information.

REFERENCES

1. C. Chen; J. Rao; Y. Tao; C. Nie; P. Xiong; Y. Xue; X. Peng; *Asia-Pacific Journal of Chemical Engineering,* **2023**, *18*, e2897.
2. Y. Zhou; X. Zhang; L. Wei; S. Liu; B. Zhang; C. Zhou; *Advances in Civil Engineering,* **2018**, *2018*, 9430517.
3. T. Chai; *Gansu Science and Technology,* **2020**, *36*, 90-92.
4. H.-S. Jung; Y.-S Han; S.-R. Chung; B.-S. Chun; Y.-J. Lee; *Tunnelling and Underground Space Technology,* **2013**, *38*, 476-486.
5. G. Atkinson; K. Raju; R. D. Howell; *SPE International Symposium on Oilfield Chemistry,* **1991**, *85*:1778.
6. Y. B. Zeng, H. M. Li; Q. H. Niu; *Journal of Jianghan Petroleum Institute*, **2001**, *23* (*2*): 56-57
7. H. R. Song; S. Y. Huang; *Carsologica Sinica,* **1990**, *9* (*2*): 105-188.
8. J. Mi; Y. G. Tang; *Resources and Environmental Engineering,* **2010**, *24* (*5*): 589-592.
9. G. P. Lu. *Journal of Mineralogy and Petrology,* **1994**, *14*, 73-78.
10. H. M. Li; S. Y. Liu; S. Xiong; H. Leng; H. Q. Chen; B. Zhang; Z. Liu. *Coatings*, **2021**, *11*, 1493.
11. X. F. Zhang; Y. F. Zhou; B. Zhang; Y. J. Zhou; S. Y. Liu. *Advances in Materials Science and Engineering,* **2018**, *2018*, 1-6.
12. R. Jain. *Conference Series*, **2022**, *35,* 1033-1047.
13. Y. Otsuka; D. Sasaki; K. Kusamori; M. Nishikawa; B. Ben-Nissan. *Coatings*, **2023**, *56*, 1373-1380.
14. K. A. Shadi; B. T. Bennett; J. P. Beck; S. Jeyapalina; T. D. Sparks. *Journal of Materials Research,* **2023**, *38*, 2287-2301.
15. V. Glauco; P. Bezerra; S. Leyliane. *Journal of Non-Crystalline Solids*, **2023**, *617*, 122494.
16. A. S. Abyzov, V. M. Fokin, E. D. Zanotto. Predicting homogeneous nucleation rates in silicate glass-formers[J]. *Journal of Non-Crystalline Solids,* **2018**, *500*: 231-234.
17. M.F. Vladimir, S.A. Alexander, S.Y. Nikolay, et al. Effect of structural relaxation on crystal nucleation in glasses[J]. *Journal of Materials Research,* **2021**, *203*: 116472.
18. T. S. Abu Haimed, S. J. Alzahrani, E. A. Attar, L. Al-Turki. Effect of Repressing Lithium Disilicate Glass Ceramics on The Shear Bond Strength of Resin Cements. *Materials,* **2023**, *16*: 6148.